Deletion of Selenoprotein P Results in Impaired Function of Parvalbumin Interneurons and Alterations in Fear Learning and Sensorimotor Gating

Matthew W. Pitts, **Arjun V. Raman**, **Ann C. Hashimoto**, **Cedomir Todorovic**, **Robert A. Nichols**, and **Marla J. Berry**

Department of Cell & Molecular Biology, John A. Burns School of Medicine, University of Hawaii, 96813

Abstract

One of the primary lines of defense against oxidative stress is the selenoprotein family, a class of proteins that contain selenium in the form of the 21st amino acid, selenocysteine. Within this class of proteins, Selenoprotein P (Sepp1) is unique, as it contains multiple selenocysteine residues and is postulated to act in selenium transport. Recent findings have demonstrated that neuronal selenoprotein synthesis is required for the development of parvalbumin (PV)-interneurons, a class of GABAergic neurons involved in the synchronization of neural activity. To investigate the potential influence of Sepp1 on PV-interneurons, we first mapped the distribution of the Sepp1 receptor, ApoER2, and parvalbumin in the mouse brain. Our results indicate that ApoER2 is highly expressed on PV-interneurons in multiple brain regions. Next, to determine whether PV-interneuron populations are affected by Sepp1 deletion, we performed stereology on several brain regions in which we observed ApoER2 expression on PV-interneurons, comparing WT and $Sepp1^{-/-}$ mice. We observed reduced numbers of PV-interneurons in the inferior colliculus of $Sepp1^{-/-}$ mice, which corresponded with a regional increase in oxidative stress. Finally, as impaired PV-interneuron function has been implicated in several neuropsychiatric conditions, we performed multiple behavioral tests on $Sepp1^{-/-}$ mice. Our behavioral results indicate that $Sepp1^{-/-}$ mice have impairments in contextual fear extinction, latent inhibition, and sensorimotor gating. In sum, these findings demonstrate the important supporting role of Sepp1 on ApoER2-expressing PV-interneurons.

Keywords

Selenoprotein P; apolipoprotein receptor 2; parvalbumin interneurons; oxidative stress; inferior colliculus

1. Introduction

Elevated oxidative stress has been implicated as a key factor in the onset and development of several neuropsychiatric disorders. One of the primary lines of defense against oxidative

Corresponding author: Dr. Matthew W. Pitts, Department of Cell & Molecular Biology, John A. Burns School of Medicine, University of Hawaii, 651 Ilalo St, Honolulu, HI, 96813, USA (mwpitts@hawaii.edu; Tel: 808-692-1516; FAX: 808-692-1968).

stress is the selenoprotein family, which include glutathione peroxidases, thioredoxin reductases, and iodothyronine deiodinases. Selenoproteins are characterized by the co-translational incorporation of selenium as selenocysteine, the 21st amino acid, at UGA codons, which typically serve as stop codons. Within this class of proteins, Selenoprotein P (Sepp1) is unique due to the fact that it contains multiple selenocysteine residues and has been postulated to act in selenium transport (Burk and Hill, 2009). In the brain, upon binding to the Apolipoprotein E receptor-2 (ApoER2) Sepp1 is taken up into neurons where it delivers selenium for selenoprotein synthesis (Burk et al., 2007). Sepp1 appears to be critically involved in brain function, as $Sepp1^{-/-}$ mice exhibit impaired hippocampal synaptic plasticity, display deficits in spatial learning, and are especially prone to seizures (Peters et al., 2006). Administration of a selenium-deficient diet to $Sepp1^{-/-}$ mice results in severe neurological dysfunction and death, whereas a high-selenium diet mitigates some, but not all, of the impairments (Hill et al., 2004; Peters et al., 2006; Burk and Hill, 2009).

Recent findings have demonstrated that neuronal selenoprotein synthesis is required for the proper function of parvalbumin (PV)-interneurons, a class of inhibitory GABAergic neurons characterized by the expression of parvalbumin (Wirth et al., 2010). These neurons coordinate brain activity by controlling the firing rates of pyramidal neurons and synchronizing spike activity within populations of neurons (Freund and Katona, 2007; Wulff et al., 2009). PV-interneurons are particularly susceptible to oxidative stress (Kinney et al., 2006; Behrens et al., 2007) and dysfunctional activity of PV-interneuron networks has been implicated in several neuropsychiatric conditions, including schizophrenia and epilepsy (Lewis et al., 2005; Freund and Katona, 2007).

We hypothesized that Sepp1 acts as a selenium transport protein to provide selenium to PV-interneurons and that deletion of Sepp1 would result in impaired PV-interneuron function. Our results indicate that the Sepp1 receptor, ApoER2, is highly expressed on PV-interneurons in multiple brain regions. In addition, $Sepp1^{-/-}$ mice exhibited diminished numbers of PV-interneurons and elevated oxidative stress in the inferior colliculus, a region involved in processing auditory information. Finally, behavioral studies revealed that $Sepp1^{-/-}$ mice display impairments in contextual fear extinction, latent inhibition, and sensorimotor gating. In sum, our findings demonstrate an important supporting role for Sepp1 in maintaining the integrity of ApoER2-expressing PV-interneurons.

2. Experimental Procedures

2.1. Animals

$Sepp1^{-/-}$ mice and $Sepp1^{+/+}$ littermates were generated from crosses of heterozygous $Sepp1^{+/-}$ mice on a C57Bl/6 background at the University of Hawaii Animal Facility. Mice were fed a selenium-adequate (0.25 mg Se/kg) diet and housed on a 12-hr/12-hr light/dark cycle. Animals were group housed until 10–12 weeks of age and then single-housed for 7–10 days to acclimatize prior to behavioral experiments. All behavioral experiments were conducted on single-housed adult mice aged 12–16 weeks during the light cycle. Experimental groups consisted of equal numbers of males and females to minimize the effect of gender. For all behavioral experiments, male and female $Sepp1^{-/-}$ mice showed similar trends when compared to gender-specific $Sepp1^{+/+}$ littermates. Thus, males and females were pooled for graphical presentation and statistical analysis. All procedures using mice were conducted under an approved University of Hawaii IACUC protocol.

2.2. Immunohistochemistry

Following behavioral testing, a representative sample (n = 6; 3 males, 3 females per group) of WT and $Sepp1^{-/-}$ mice were selected for immunohistochemistry. Mice were deeply anesthetized (1.2% avertin; 0.7 ml/mouse) and perfused with ice cold 0.1M phosphate-

buffered saline (PBS) followed by 4% paraformaldehye (PFA) in PBS. Brains were removed, stored in 4% PFA for 24-hr, and immersed in graded solutions of sucrose (10%, 20%, 30%) until sunk. Brains were cut into 40 μm sections and stored in a cryoprotective solution (0.05M PBS, 25% glycerol, 25% polyethylene glycol) at 4°C. For DAB immunohistochemistry, free-floating sections were treated with 0.3% H_2O_2 to inactivate endogenous peroxidases, blocked, and incubated overnight at 4°C with the proper primary antibody. The next day, sections were probed with the appropriate biotinylated secondary antibody followed by incubation in avidin-biotin-peroxidase complex (Vector ABC Kit, Vector Labs), and immunoreactivity was visualized by peroxidase detection using diaminobenzidine tetrahydrochloride (DAB; DAB Substrate Kit, Vector Labs) as a chromogen substrate. After several rinses in PBS, sections were mounted on slides, dehydrated with graded solutions of EtOH followed by xylene, and coverslipped. For immunofluorescence, a similar procedure was used, except that the sections were not incubated with H_2O_2 and appropriate Alexafluor-labeled fluorescent secondary antibodies were used for visualization instead of DAB.

2.3. Antibodies

The primary antibodies used in these studies were as follows: rabbit anti-parvalbumin (1:10,000; Swant, PV 25), rabbit anti-calretinin (1:2000; Swant, CR 7699), rabbit anti-calbindin (1:2000; Swant, CB38), goat anti-ApoER2 (1:50; Santa Cruz, sc-10113), mouse anti-GAD67 (1:5000; Millipore, MAB5406) and mouse anti-8-oxo-dG (1:250; QED Bioscience, 12501). In addition, we also used an ApoER2 blocking peptide (1:25; Santa Cruz, sc-10113 P) to verify the specificity of our anti-ApoER2 antibody.

2.4. Stereology

Quantitative analysis of cell numbers was performed on a Zeiss Axioskop microscope equipped with MicroBrightfield Stereo Investigator software (MBF Bioscience). An optical dissector (counting box) was used to analyze and count neurons. The following regions were outlined using a 5x objective with the aid of a mouse brain atlas (Paxinos & Franklin, 2004) at specified coronal levels relative to bregma: somatosensory cortex (1.18); medial septum (0.50); CA1, CA2/3, and DG of the dorsal hippocampus (−1.82); and inferior colliculus (−5.02). Following contour selection, an optical fractionator analysis was conducted at high magnification (20x objective) using a 300 μm x 300 μm counting frame to quantify the number of positive neurons. For each counting site, the mounted section thickness was determined. Mean section thickness was calculated by averaging all counting sites from each section and this value was used to determine the number of immunopositive numbers per unit volume.

2.5. Quantification of 8-oxo-dG immunoreactivity

The density of the 8-oxo-dG immunoreactivity in the inferior colliculus was quantified at the same coronal level (−5.02) as used for stereology. Images were acquired using a 5x objective lens under identical light intensity and exposure times. Black and white images were imported into ImageJ 1.37c and inverted to simulate dark-field illumination. For each image, contours were drawn around the inferior colliculus and the adjacent lateral periaqueductal gray (LPAG). The contour surrounding the inferior colliculus selected for positive 8-oxo-dG immunoreactivity while the adjacent LPAG acted as a background control region. Mean optical density numbers were derived by subtracting the LPAG optical density measurements from those obtained for the inferior colliculus.

2.6. Confocal imaging

Z-stack images were acquired using a Zeiss LSM 5 Pascal imaging system and consisted of 10 individual stacks collected at intervals of 1 μm. Images were then imported into NIH ImageJ and converted into Z-stack projection images for two dimensional presentation.

2.7. Contextual fear conditioning

For the acquisition of contextual fear, mice were placed in a computer-controlled fear conditioning system (TSE Systems) for a 6-min conditioning trial. Following a 2-min exploratory period, two electric footshocks (0.8 mA, 2-s duration, constant current) were delivered through a stainless steel grid floor at 2-min intervals. During each 2-min post-shock interval, freezing was measured. At the conclusion of conditioning, mice were returned to their home cages. After 24-hr, mice were returned to the conditioning apparatus for a 4-min contextual fear retention test during which freezing was measured and no footshocks were delivered. To test for fear extinction, contextual fear retention was then assessed for an additional 3 consecutive days. Two weeks after the final extinction test, mice were again returned to the conditioning apparatus for an additional 4-min contextual fear retention test to assess spontaneous recovery (Rescorla, 2004).

2.8. Latent inhibition

Latent inhibition was investigated using a conditioned freezing paradigm in the same apparatus used for contextual fear conditioning. As previous exposure to the conditioning apparatus could confound latent inhibition, the mice used for this study had not been used for any prior conditioning procedures and thus were naïve to the apparatus. Our latent inhibition paradigm consisted of 4 phases: exposure, conditioning, contextual retention test, and tone retention test. Animals from each genotype were randomly allocated to either exposed (E) or non-exposed (NE) groups. For three consecutive days, group E was placed in the fear conditioning apparatus and received 20 presentations of a 20-s tone stimulus (75 dB, pulsed 5 Hz) with 25-s inter-stimulus intervals. Group NE was placed in the conditioning apparatus for an equal amount of time (15-min), but no tones were administered. On day 3, immediately following the 15-min pre-exposure trial, both groups of mice remained in the apparatus for conditioning. The conditioning trial consisted of an initial 2-min exploration period followed by two tone-footshock pairings (2-s, 0.8 mA), with a 2-min interval between pairings and concluded 2-min after the second footshock. To assess fear acquisition, freezing was measured during each 2-min post-shock interval. On day 4, mice were returned to the conditioning apparatus for a 4-min contextual fear retention test and freezing was measured. On day 5, mice were placed in a novel chamber for the tone retention test. Following an initial 2-min exploratory period in the novel chamber, the tone was continuously presented for 4-min during which freezing was assessed.

2.9. Acoustic startle and prepulse inhibition

Mice were placed in the startle chamber (Responder-X, Columbus Instruments) and allowed a 5-min acclimation period with the background noise (70 dB) continually present. Immediately following the acclimation period, two blocks of trials were administered to assess the acoustic startle response and prepulse inhibition, respectively. The first block of trials consisted of 8 sets of 8 types of trials that were randomly distributed. Startle stimuli (40-ms) of varying intensities were administered, with an inter-stimulus interval of 15-s. The stimulus intensities were 80, 85, 90, 95, 100, 105, and 110 dB. In addition, to assess baseline activity, a set of no-stimulus trials were included. Measures were taken of the startle amplitude for each trial, defined as the peak response during a 100-ms sampling window beginning with the onset of the startle stimulus. Mean startle amplitudes were derived by subtracting the average startle amplitude from the no-stimulus trial (70 dB) from the average

startle amplitude for each stimulus intensity tested (80 – 110 dB). In addition, mean startle amplitudes were normalized for body weight by dividing the mean startle amplitude by the subject's body weight. This added measure was taken to limit variability due to gender, as females had both lower mean startle amplitudes and lower body weights. The second block of trials consisted of 8 sets of 5 trial types, distributed randomly and separated by 20-s inter-stimulus intervals. The trial types were as follows: 1) no-stimulus/background noise (70 dB); 2) 40-ms, 110 dB startle alone; 3–5) 110 dB startle preceded 100-ms by one of three 20-ms prepulses at the following intensities: 74 dB, 78 dB, 86 dB. The startle amplitude for each subject at each of the different prepulse intensities was calculated as follows: PPI = 100 – 100 x [response amplitude for prepulse stimulus paired with startle stimulus / response amplitude for startle stimulus alone]. For our PPI calculations, the response amplitude for the startle stimulus alone was derived by averaging the 110 dB startle stimulus across the acoustic startle and prepulse inhibition sessions. In addition, we ran 12 animals per gender for each genotype, but several animals with low startle amplitudes produced highly variable values for PPI. Thus, in order limit variability for PPI, we selected the 8 males and 8 females from each genotype with the median values for startle amplitude at 110 dB for statistical analysis and graphical presentation. As this procedure involves loud auditory stimuli and could potentially confound other behavioral procedures, this test was always performed last when animals were used for multiple tests.

3. Results

3.1. ApoER2 is highly expressed on PV-interneurons

There is evidence that parvalbumin (PV)-interneurons are particularly sensitive to oxidative stress (Behrens et al., 2007; Behrens et al., 2008; Wang et al., 2011) and recently selenoprotein synthesis has been implicated as a critical factor for the function of this important class of interneurons (Wirth et al., 2010). However, the functional relationship between the putative selenium transport protein, Selenoprotein P (Sepp1), and PV-interneurons has not been clearly defined. Therefore, using immunohistochemistry, we mapped out the expression profiles of the Sepp1 receptor, ApoER2, and parvalbumin (PV) in the mouse brain to evaluate the potential influence of Sepp1 on PV-interneurons. First, to verify the specificity of our ApoER2 antibody, we preincubated tissue sections with an ApoER2 blocking peptide and observed an absence of signal over background (Fig. 1A). Next, to determine whether ApoER2 is expressed on PV-interneurons, we used multi-label immunofluorescence. Confocal images show that ApoER2 is expressed on PV-interneurons in several brain regions, including the somatosensory cortex (Fig. 1B), hippocampus (Fig. 1C), inferior colliculus (Fig. 1D), medial septum, red nucleus, reticular thalamus, and cerebellum (others not shown). To assess whether ApoER2 is expressed on other classes of interneurons, we also examined ApoER2 expression relative to calretinin (CR) and calbindin (CB), markers for two additional classes of GABAergic interneurons. In contrast to the widespread expression of ApoER2 that we observed on PV-interneurons, ApoER2 did not appear to co-localize with either calretinin (Fig. 2A, B) or calbindin (Fig. 2C, D) in any of the regions investigated.

3.2. Reduced density of PV-interneurons in *Sepp1$^{-/-}$* mice

We next sought to determine whether *Sepp1$^{-/-}$* mice have diminished numbers of PV-interneurons. Our investigation focused upon four brain regions in which we observed ApoER2 expression on PV-interneurons: the somatosensory cortex (SC), medial septum (MS), hippocampus, and inferior colliculus (IC) (Fig. 3). The septohippocampal regions were selected based upon previous results demonstrating that Sepp1 deletion results in impaired spatial learning and hippocampal synaptic plasticity (Peters et al., 2006). We also chose to examine the somatosensory cortex and inferior colliculus because these regions

were shown to be especially prone to neurodegeneration when $Sepp1^{-/-}$ mice are fed a selenium-deficient diet (Valentine et al., 2008; Caito et al., 2011). Two-way ANOVA analysis revealed a significant main effect for brain region ($F_{(5, 60)} = 60.46$, $p<0.0001$), a significant reduction of PV-interneuron density in $Sepp1^{-/-}$ mice ($F_{(1, 10)} = 6.835$, $p<0.05$), and a significant brain region x genotype interaction ($F_{(5, 60)} = 2.383$, $p<0.05$). Post-hoc tests indicated that the reduction of PV-interneuron density in $Sepp1^{-/-}$ mice was greatest in the inferior colliculus ($t_{10} = 3.730$, $p<0.01$). In contrast, the density of calretinin-(CR) interneurons within the inferior colliculus did not differ between genotypes (WT $Sepp1^{+/+} =$ 10310 ± 1726, $Sepp1^{-/-} = 10330 \pm 587.6$; $t_{10} = 0.01079$, $p>0.05$) (Fig. 3C).

3.3. Elevated oxidative stress in the inferior colliculus of $Sepp1^{-/-}$ mice

To assess whether the observed reduction of PV-interneuron density in the inferior colliculus may be related to a regional increase in oxidative stress, we probed brain sections from WT $Sepp1^{+/+}$ and $Sepp1^{-/-}$ mice for 8-oxo-2'-deoxyguanosine (8-oxo-dG), a marker of oxidative damage to DNA and RNA. Oxidative damage was elevated in $Sepp1^{-/-}$ mice ($t_{22} = 2.080$, $p<0.05$) (Fig. 4A, B) and this increase appeared to correspond with a reduction in PV expression. This notion was further confirmed using double-label immunohistochemistry to illustrate the correlation of diminished PV levels with increased 8-oxo-dG staining in $Sepp1^{-/-}$ mice (Fig. 4C).

3.4. Enhanced acquisition and impaired extinction of contextual fear memory in Sepp1$^{-/-}$ mice

As PV-interneuron dysfunction has been implicated in human neuropsychiatric conditions, we tested $Sepp1^{-/-}$ mice on several behavioral assays. Previous studies on $Sepp1^{-/-}$ mice fed a high selenium diet reported impaired hippocampal synaptic plasticity and deficits in spatial learning, while contextual fear memory appeared normal (Peters et al., 2006). We first re-examined contextual fear acquisition and retention in our $Sepp1^{-/-}$ mice fed a standard, selenium-adequate lab diet. In addition, we also assessed fear retention over several consecutive days to evaluate fear extinction. Two-way ANOVA analysis of freezing behavior during conditioning revealed a significant main effect for shock interval ($F_{(2, 78)} = 85.69$, $p<0.0001$), significantly elevated freezing in $Sepp1^{-/-}$ mice ($F_{(1, 26)} = 28.75$, $p<0.0001$), and a significant genotype x shock interval interaction ($F_{(2, 78)} = 5.184$, $p<0.01$) (Fig. 5B). Post-hoc tests showed significant differences in freezing during the first ($t_{26} = 5.865$, *$p<0.001$) but not second, post-shock interval between groups. For contextual fear retention, we observed a significant main effect for retention test day ($F_{(4, 130)} = 3.386$, $p<0.05$), significantly increased levels of freezing in $Sepp1^{-/-}$ mice ($F_{(1, 26)} = 21.1$, $p<0.0001$), and a non-significant test day x genotype interaction ($p>0.05$) (Fig. 5C). Post-hoc tests revealed that the difference in freezing levels between genotypes was highest on the 96-hr retention test ($t_{26} = 3.564$, *$p<0.01$). When mice were tested for spontaneous recovery of fear memory 18 days after initial conditioning, wild-type mice froze at levels comparable to the initial retention test (24-hr) and no significant differences were found between genotypes. In sum, these results indicate that $Sepp1^{-/-}$ mice exhibit enhanced initial acquisition and delayed extinction of contextual fear memory.

3.5. Absence of latent inhibition in $Sepp1^{-/-}$ mice

To further assess the effects of Sepp1 deletion on behavior, we next examined latent inhibition using a similar conditioned freezing paradigm (Fig. 6A). Latent inhibition is a measure of reduced association to a stimulus in which there has been previous exposure without any consequences. Development of latent inhibition reflects a process of learning to ignore, or tune out, irrelevant stimuli (Lubow and Moore, 1959).

Animals from each genotype were divided into exposed (E) or non-exposed (NE) groups. Exposed (E) animals were placed into the contextual fear conditioning apparatus for 15-min on 3 consecutive days during which they were repeatedly exposed to a tone. In contrast, non-exposed (NE) animals were placed in the conditioning apparatus for an equal amount of time during which no tones were administered. On day 3, immediately following the 15-min exposure trial, animals were subjected to a fear conditioning procedure exactly as previously performed, except that a tone immediately preceded the footshock. During the conditioning trial, no significant effects were observed for genotype or exposure condition (Fig 6B). Twenty-four hours after conditioning (Day 4), animals were returned to the fear conditioning apparatus and contextual fear retention was evaluated (Fig. 6C). Two-way ANOVA analysis revealed a significant main effect for exposure condition ($F_{(1, 38)} = 5.192$, $p < 0.05$), but not for genotype. The genotype x exposure interaction was also not significant. On the following day (Day 5), animals were placed in a novel context and given a 4-min tone to assess auditory fear retention (Fig. 6D). Mice in the exposed (E) group displayed significantly less freezing than their non-exposed (NE) counterparts ($F_{(1, 38)} = 11.57$, $p < 0.01$). A significant exposure condition x genotype was observed ($F_{(1, 38)} = 20.52$, $p < 0.0001$), whereas there was the main effect for genotype was non-significant ($p > 0.05$). Post-hoc tests demonstrated that exposed (E) WT mice froze at significantly lower levels than non-exposed (NE) WT mice ($t_{18} = 5.608$, $*p < 0.001$). In contrast, there was no trend toward diminished freezing in exposed (E) $Sepp1^{-/-}$ mice when compared to non-exposed (NE) $Sepp1^{-/-}$ mice. These results demonstrate that in our latent inhibition paradigm, exposure to the tone prior to conditioning produced latent inhibition in the $Sepp1^{+/+}$ but not $Sepp1^{-/-}$ mice.

3.6. Diminished acoustic startle reactivity and prepulse inhibition in $Sepp1^{-/-}$ mice

One behavioral endophenotype associated with a variety of mental illnesses is dysfunctional sensorimotor gating, which is generally assessed by measuring prepulse inhibition (PPI) of the acoustic startle reflex (Braff et al., 2001). In order to evaluate sensorimotor gating, we first measured acoustic startle reactivity to stimuli of varying intensities (80 –110 dB) and then evaluated the degree of inhibition elicited when a prepulse (4, 8, or 16 dB above background) immediately preceded the highest intensity startle stimulus (110 dB).

In response to stimuli of increasing magnitude, both $Sepp1^{-/-}$ and WT littermates showed progressively elevated startle amplitudes ($F_{(6, 322)} = 49.01$, $p < 0.0001$) (Fig. 7A). $Sepp1^{-/-}$ mice exhibited a reduced startle response in comparison to WT littermates ($F_{(1, 46)} = 16.58$, $p < 0.0001$) and the stimulus intensity x genotype interaction was also significant ($F_{(6, 322)} = 2.484$, $p < 0.05$). The difference in startle reactivity between genotypes was most pronounced at the highest stimulus intensity (110 dB) ($t_{46} = 4.922$, $*p < 0.001$). When tested for prepulse inhibition immediately following the acoustic startle test, we observed elevated degrees of prepulse inhibition in response to louder prepulse intensities ($F_{(2, 90)} = 9.668$, $p < 0.001$) (Fig. 7B). In addition, prepulse inhibition was significantly reduced in $Sepp1^{-/-}$ mice in comparison to WT controls ($F_{(1, 90)} = 7.831$, $p < 0.01$). Post-hoc tests showed that the difference in prepulse inhibition between genotypes was greatest when the prepulse intensity was 16 dB above background ($t_{30} = 2.656$, $*p < 0.05$). These data indicate that $Sepp1^{-/-}$ mice display a diminished startle response to high intensity acoustic stimuli and exhibit deficits in prepulse inhibition.

4. Discussion

In summary, our main findings are as follows: First, the Sepp1 receptor, ApoER2, is highly expressed on PV-interneurons. Second, Sepp1 deletion results in elevated oxidative damage and diminished PV expression in the inferior colliculus. Finally, behavioral studies showed

that $Sepp1^{-/-}$ mice exhibit impairments in contextual fear extinction, latent inhibition, and sensorimotor gating.

ApoER2 is a multifunctional member of the low-density lipoprotein (LDL) receptor family that binds apolipoprotein E, reelin, and Sepp1. We observed high levels of ApoER2 expression on PV-interneurons relative to other classes of neurons. In contrast to an earlier study (Clatworthy et al., 1999), we observed relatively low levels of ApoER2 expression in granule cells of the dentate gyrus and pyramidal neurons of the hippocampus. This observed difference may be due to the ApoER2 antibodies used for each study. Our antibody targets the C-terminal portion of the ApoER2 protein, a region that is known to be alternatively spliced (Kim et al., 1997; Clatworthy et al., 1999). This antibody could potentially target an ApoER2 splice variant that is more selectively expressed on PV-interneurons.

Within the brain, ApoER2 is the primary receptor for Sepp1 (Burk et al., 2007). Both $ApoER2^{-/-}$ and $Sepp1^{-/-}$ mice have significantly reduced brain selenium levels and exhibit severe neurological dysfunction under conditions of selenium deficiency (Burk et al., 2007; Burk and Hill, 2009). Concurrent with the diminished selenium levels, the activity of the selenium-containing antioxidant enzymes of the glutathione peroxidase and thioredoxin reductase families are decreased in the brains of $Sepp1^{-/-}$ mice (Schomburg et al., 2003; Hill et al., 2004). Furthermore, $ApoER2^{-/-}$ and $Sepp1^{-/-}$ mice fed a selenium-deficient diet display extensive neurodegeneration in several brain regions associated with auditory and motor function (Valentine et al., 2008). One region that showed severe neurodegeneration in both of the aforementioned genotypes was the inferior colliculus, suggesting that ApoER2-mediated uptake of Sepp1 serves an important neuroprotective role in this brain region.

Our results build upon these findings and suggest that Sepp1 deletion renders PV-interneurons particularly susceptible to oxidative stress within the inferior colliculus. The inferior colliculus is the primary midbrain nucleus of the auditory pathway, plays a critical role in processing auditory information, and has been reported to be the most metabolically active brain region (Sokoloff et al., 1981; Jay et al., 1988). Extensive research by Brandão and colleagues has shown that GABAergic mechanisms within the inferior colliculus regulate both defensive behavior and auditory gating (Brandão et al., 2005). Both site-specific infusions of the GABA receptor antagonist, bicuculline, and direct electrical stimulation of the rat inferior colliculus elicit defensive behavior, such as escape and freezing (Brandão et al., 1988; Lamprea et al., 2002). Additional studies showed that microinfusions of semicarbazide, an inhibitor of the enzyme responsible for GABA synthesis, at doses that induced freezing, also enhanced auditory evoked potentials and impaired the acoustic startle response (Nobre et al., 2003). Further work has demonstrated that the inferior colliculus exerts a modulatory influence on prepulse inhibition (PPI), as both lesions (Li et al., 1998) and electrical stimulation (Silva et al., 2005) have been shown to impair PPI. Finally, diminished GABA-mediated inhibition within the inferior colliculus has been reported in genetically epilepsy prone rats (Faingold et al., 1986; Faingold & Anderson, 1991) and decreased inhibition within this region is thought to increase susceptibility to audiogenic seizures (Faingold, 2002). In sum, these results are consistent with our finding that the behavioral deficits observed in $Sepp1^{-/-}$ mice are associated with impaired GABAergic function of the inferior colliculus.

The possibility exists that some of the behavioral deficits (latent inhibition, auditory gating) observed in $Sepp1^{-/-}$ mice may be due to impairments in hearing. Of particular relevance, mice lacking the type 2 iodothyronine deiodinase (Dio2), a known selenoprotein, exhibit impaired cochlear development and hearing loss (Ng et al., 2004). Furthermore, in humans, mutations in the SECIS binding protein 2, a selenocysteine-specific translation elongation factor, lead to decreased Dio2 activity (Dumitrescu et al., 2005). A clinical study on two

human patients with this rare mutation reported a multisystem disorder including hearing loss (Schoenmakers et al., 2010). Nevertheless, the fact that the acoustic startle magnitudes differed most between genotypes at the highest, rather than lowest, sound intensities suggest that $Sepp1^{-/-}$ mice exhibit deficits in auditory processing rather than auditory perception. This notion is corroborated by previous findings that auditory fear conditioning is normal in $Sepp1^{-/-}$ mice (Peters et al., 2006).

Accumulating evidence has shown that PV-interneurons are particularly vulnerable to redox dysregulation (Kinney et al., 2006; Behrens et al., 2007; Steullet et al., 2010; Wang et al., 2011) and impairments in PV-interneuron function due to oxidative stress are hypothesized to be a contributing factor to schizophrenia (Behrens and Sejnowski, 2009; Do et al., 2009; Bitanihirwe and Woo, 2011). Additionally, deficits in fear extinction (Holt et al., 2009), latent inhibition (Baruch et al., 1988; Kathmann et al., 2000), and prepulse inhibition (Braff et al., 2001) have been reported in patients with schizophrenia. However, in human studies, reduced PV expression has been observed largely in the prefrontal cortex (Lewis et al., 2005), a region in which we observed low levels of ApoER2 expression. Further studies are needed to clarify whether impairments in selenoprotein synthesis and function contribute to schizophrenia.

Prior to this study, it was shown that neuronal selenoprotein synthesis is required for the proper development of PV-interneurons (Wirth et al., 2010). Our results indicate that the Sepp1 receptor, ApoER2, is strongly expressed on PV-interneurons, suggesting selective targeting of Sepp1 to this particular class of neurons. Based upon our current findings and the existing literature, we propose the following model of PV-interneuron function and oxidative stress (Fig. 8). Sepp1 binds to ApoER2 and provides selenium for selenoprotein synthesis within PV-interneurons. Selenoproteins, particularly glutathione peroxidase 4 (GPx4) which appears to be essential (Yant et al., 2003, Wirth et al., 2010), protect against oxidative stress. Elevated oxidative stress results in diminished expression of parvalbumin (Kinney et al., 2006; Wang et al., 2011) and impaired NMDA-mediated neurotransmission (Kohr et al., 1994; Steullet et al., 2006). Also included in this model, but beyond the scope of this investigation, are two additional ligands for the ApoER2 receptor, APOE and reelin.

5. Conclusion

This report details the neuroprotective role of ApoER2-mediated uptake of Sepp1 on PV-interneurons. We hypothesize that the behavioral deficits we observed, as well as those previously reported (Hill et al., 2004; Peters et al., 2006), are largely due to diminished integrity of PV-interneuron networks. Previous studies (Valentine et al., 2008) and our findings together indicate that ApoER2-mediated uptake of Sepp1 serves an important neuroprotective role in the inferior colliculus. Yet, the observed deficits apparent in these mice may also be influenced by dysfunctional activity in other brain regions containing ApoER2-expressing PV-interneurons, such as the hippocampus, medial septum, reticular thalamus, red nucleus, cerebellum, and the cingulate, retrosplenial, and somatosensory cortices. These findings may have relevance to neuropsychiatric conditions in which dysfunctional PV-interneuron networks have been implicated, such as epilepsy and schizophrenia.

Acknowledgments

References

Baruch I, Hemsley DR, Gray JA. Differential performance of acute and chronic schizophrenics in a latent inhibition task. J Nerv Ment Dis. 1988; 176:598–606. [PubMed: 2903219]

Behrens MM, Ali SS, Dao DN, Lucero J, Shekhtman G, Quick KL, Dugan LL. Ketamine-induced loss of phenotype of fast-spiking interneurons is mediated by NADPH-oxidase. Science. 2007; 318:1645–1647. [PubMed: 18063801]

Behrens MM, Ali SS, Dugan LL. Interleukin-6 mediates the increase in NADPH oxidase in the ketamine model of schizophrenia. J Neurosci. 2008; 28:13957–18966. [PubMed: 19091984]

Behrens MM, Sejnowski TJ. Does schizophrenia arise from oxidative dysregulation of parvalbumin-interneurons in the developing cortex? Neuropharmacology. 2009; 57:193–200. [PubMed: 19523965]

Bitanihirwe BK, Woo TU. Oxidative stress in schizophrenia: an integrated approach. Neurosci Biobehav Rev. 2011; 35:878–893. [PubMed: 20974172]

Brandão ML, Tomaz C, Borges PC, Coimbra NC, Bagri A. Defense reaction induced by microinjections of bicuculline into the inferior colliculus. Physiol Behav. 1988; 44:361–365. [PubMed: 2851846]

Brandão ML, Borelli KG, Nobre MJ, Santos JM, Albrechet-Souza L, Oliveira AR, Martinez RC. Gabaergic regulation of the neural organization of fear in the midbrain tectum. Neurosci Biobehav Rev. 2005; 29:1299–1311. [PubMed: 16084589]

Braff DL, Geyer MA, Swerdlow NR. Human studies of prepulse inhibition of startle: Normal subjects, patient groups, and pharmacological studies. Psychopharmacology (Berl). 2001; 156:234–258. [PubMed: 11549226]

Burk RF, Hill KE, Olson GE, Weeber EJ, Motley AK, Winfrey VP, Austin LM. Deletion of apolipoprotein E receptor-2 in mice lowers brain selenium and causes severe neurological dysfunction and death when a low-selenium diet is fed. J Neurosci. 2007; 27:6207–6211. [PubMed: 17553992]

Burk RF, Hill KE. Selenoprotein P – Expression, functions, and roles in mammals. Biochim Biophys Acta. 2009; 1790:1441–1447. [PubMed: 19345254]

Caito SW, Milatonic D, Hill KE, Aschner M, Burk RF, Valentine WM. Progression of neurodegeneration and morphologic changes in the brains of juvenile mice with selenoprotein P deleted. Brain Res. 2011; 1398:1–12. [PubMed: 21636077]

Clatworthy AE, Stockinger W, Christie RH, Schneider WJ, Nimpf J, Hyman BT, Rebeck GW. Expression and alternate splicing of apolipoprotein receptor 2 in brain. Neuroscience. 1999; 90:903–911. [PubMed: 10218790]

Do KQ, Cabungcal JH, Frank A, Steullet P, Cuenod M. Redox dysregulation, neurodevelopment, and schizophrenia. Curr Opin Neurobiol. 2009; 19:220– 230. [PubMed: 19481443]

Dumitrescu AM, Liao XH, Abdullah MS, Lado-Abeal J, Majed FA, Moeller LC, Boran G, Schomburg L, Weiss RE, Refetoff S. Mutations in SECISBP2 result in abnormal thyroid metabolism. Nat Genet. 2005; 37:1247–1252. [PubMed: 16228000]

Faingold CL, Gehlbach G, Caspary DM. Decreased effectiveness of GABA- mediated inhibition in the inferior colliculus of the genetically epilepsy-prone rat. Exp Neurol. 1986; 93:145–159. [PubMed: 3732456]

Faingold CL, Anderson CA. Loss of intensity-induced inhibition in inferior colliculus neurons leads to audiogenic seizure susceptibility in behaving genetically epilepsy-prone rats. Exp Neurol. 1991; 113:354–363. [PubMed: 1915725]

Faingold CL. Role of GABA abnormalities in the inferior colliculus pathophysiology - audiogenic seizures. Hear Res. 2002; 168:223–237. [PubMed: 12117523]

Freund TF, Katona I. Perisomatic inhibition. Neuron. 2007; 56:33–42. [PubMed: 17920013]

Hill KE, Zhou J, McMahan WJ, Motley AK, Burk RF. Neurological dysfunction occurs in mice with targeted deletion of the selenoprotein P gene. J Nutr. 2004; 134:157–161. [PubMed: 14704310]

Holt DJ, Lebron-Milad K, Milad MR, Rauch SL, Pitman RK, Orr SP, Cassidy BS, Walsh JP, Goff DC. Extinction memory is impaired in schizophrenia. Biol Psychiatry. 2009; 65:455–63. [PubMed: 18986648]

Jay TM, Lucignani G, Crane AM, Jehle J, Sokoloff. Measurement of local cerebral blood flow with [14C]iodoantipyrine in the mouse. J Cereb Blood Flow Metab. 1988; 8:121–129. [PubMed: 3339102]

Kathmann N, von Recum S, Haag C, Engel RR. Electrophysiological evidence for reduced latent inhibition in schizophrenic patients. Schizophr Res. 2000; 45:103–114. [PubMed: 10978878]

Kim DH, Magoori K, Inoue TR, Mao CC, Kim HJ, Suzuki H, Fujita T, Endo Y, Saeki S, Yamamoto TT. Exon/intron organization, chromosome localization, alternative splicing, and transcription units of the human apolipoprotein E receptor 2 gene. J Biol Chem. 1997; 272:8498–8504. [PubMed: 9079678]

Kinney JW, Davis CN, Tabarean I, Conti B, Bartfai T, Behrens MM. A specific role for NR2A-containing NMDA receptors in the maintenance of parvalbumin and GAD67 immunoreactivity in cultured interneurons. J Neurosci. 2006; 26:1604–1615. [PubMed: 16452684]

Kohr G, Eckardt S, Luddens H, Monyer H, Seeburg PH. NMDA receptor channels: subunit-specific potentiation by reducing agents. Neuron. 1994; 12:1031–1040. [PubMed: 7514425]

Lamprea MR, Cardenas FP, Vianna DM, Castilho VM, Cruz-Morales SE, Brandão ML. The distribution of fos immunoreactivity in rat brain following freezing and escape responses elicited by electrical stimulation of the inferior colliculus. Brain Res. 2002; 950:186–94. [PubMed: 12231243]

Lewis DA, Hashimoto T, Volk DW. Cortical inhibitory neurons and schizophrenia. Nat Rev Neurosci. 2005; 6:312–324. [PubMed: 15803162]

Li L, Korngut LM, Frost BJ, Beninger RJ. Prepulse inhibition following lesions of the inferior colliculus: prepulse intensity functions. Physiol Behav. 1998; 65:133–139. [PubMed: 9811375]

Lubow RE, Moore AU. Latent inhibition: The effect of nonreinforced preexposure. J Comp Physiol Psychol. 1959; 52:415–419. [PubMed: 14418647]

Ng L, Goodyear RJ, Woods CA, Schneider MJ, Diamond E, Richardson GP, Kelley MW, Germain DL, Galton VA, Forrest D. Hearing loss and retarded cochlear development in mice lacking type 2 iodothyronine deiodinase. Proc Natl Acad Sci USA. 2004; 101:3474–3479. [PubMed: 14993610]

Nobre MJ, Sandner G, Brandão ML. Enhancement of acoustic evoked potentials and impairment of startle reflex induced by reduction of GABAergic control of the neural substrates of aversion in the inferior colliculus. Hear Res. 2003; 184:82–90. [PubMed: 14553906]

Paxinos, G.; Franklin, K. The mouse brain in stereotaxic coordinates. 2. Elsevier Academic Press; 2004.

Peters MM, Hill KE, Burk RF, Weeber EJ. Altered hippocampus synaptic function in selenoprotein P deficient mice. Mol Neurodegener. 2006 Sep 19.:1–12.

Rescorla RA. Spontaneous recovery. Learn Mem. 2004; 11:501–509. [PubMed: 15466300]

Schoenmakers E, Agnostini M, Mitchell C, Schoenmakers E, Papp L, Rajanayagam O, Padidela R, Ceron-Gutierrez L, Doffinger R, Prevosto C, Luan J, Montano S, Lus J, Castanet M, Clemons N, Groeneveld M, Castets P, Karbaschi M, Aitken S, Dixon A, Williams J, Campi I, Blount M, Burton H, Muntoni F, O'Donovan D, Dean A, Warren A, Brierley C, Baguley D, Guicheney P, Fitzgerald R, Coles A, Gaston H, Todd P, Holmgren A, Khanna KK, Cooke M, Semple R, Halsall D, Wareham N, Schwabe J, Grasso L, Beck-Peccoz P, Ogunko A, Dattani M, Gurnell M, Chatterjee K. Mutations in the selenocysteine insertion sequence-binding protein 2 gene lead to a multisystem selenoprotein deficiency disorder in humans. J Clin Invest. 2010; 120:4220–4235. [PubMed: 21084748]

Schomburg L, Schweizer U, Holtmann B, Flohe L, Sendtner M, Kohrle J. Gene disruption discloses the role of selenoprotein P in selenium delivery to target tissues. Biochem J. 2003; 370:397–402. [PubMed: 12521380]

Silva RC, Sandner G, Brandão ML. Unilateral electrical stimulation of the inferior colliculus of rats modifies the prepulse modulation of the startle response (PPI): effects of ketamine and diazepam. Behav Brain Res. 2005; 160:323–330. [PubMed: 15863228]

Sokoloff L. Localization of functional activity in the central nervous system by measurement of glucose utilization with radioactive deoxyglucose. J Cereb Blood Flow Metabol. 1981; 1:7–36.

Steullet P, Neijt HC, Cuenod M, Do KQ. Synaptic plasticity impairment and hypofunction of NMDA receptors induced by glutathione deficit: Relevance to schizophrenia. Neuroscience. 2006; 137:807–819. [PubMed: 16330153]

Steullet P, Cabungcal JH, Kulak A, Kraftsik R, Chen Y, Dalton TP, Cuenod M, Do KQ. Redox dysregulation affects the ventral but not dorsal hippocampus: impairment of parvalbumin neurons, gamma oscillations, and related behaviors. J Neurosci. 2010; 30:2547–2558. [PubMed: 20164340]

Valentine WM, Abel TW, Hill KE, Austin LM, Burk RF. Neurodegeneration in mice resulting from loss of functional selenoprotein P or its receptor apolipoprotein E receptor 2. J Neuropathol Exp Neurol. 2008; 67:68–77. [PubMed: 18172410]

Wang X, Zhou Z, Yang C, Xu J, Yang J. Nuclear factor-κB is involved in the phenotype loss of parvalbumin-interneurons *in vitro*. Neuroreport. 2011; 22:264–268. [PubMed: 21378588]

Wirth EK, Conrad M, Winterer J, Wozny C, Carlson BA, Roth S, Schmitz D, Bornkamm GW, Coppola V, Tessarollo L, Schomburg L, Kohrle J, Hatfield DL, Schweizer U. Neuronal selenoprotein expression is required for interneuron development and prevents seizures and neurodegeneration. FASEB J. 2010; 24:844–852. [PubMed: 19890015]

Wulff P, Ponomarenko AA, Bartos M, Korotkova TM, Fuchs EC, Bahner F, Both M, Tort ABL, Kopell NJ, Wisden W, Monyer H. Hippocampal theta rhythm and its coupling with gamma oscillations require fast inhibition onto parvalbumin-positive interneurons. Proc Natl Acad Sci USA. 2009; 106:3561–3566. [PubMed: 19204281]

Yant LJ, Ran Q, Rao L, Van Remmen H, Shibatani T, Belter JG, Motta L, Richardson A, Prolla TA. The selenoprotein GPX4 is essential for mouse development and protects from radiation and oxidative damage insults. Free Radic Biol Med. 2003; 34:496–502. [PubMed: 12566075]

Research Highlights

- The receptor for Selenoprotein P (Sepp1), ApoER2, is highly expressed on parvalbumin (PV)-interneurons.

- $Sepp1^{-/-}$ mice have reduced numbers of PV-interneurons in the inferior colliculus, which corresponds with a regional increase in oxidative stress.

- $Sepp1^{-/-}$ mice display deficits in contextual fear extinction, latent inhibition, and sensorimotor gating.
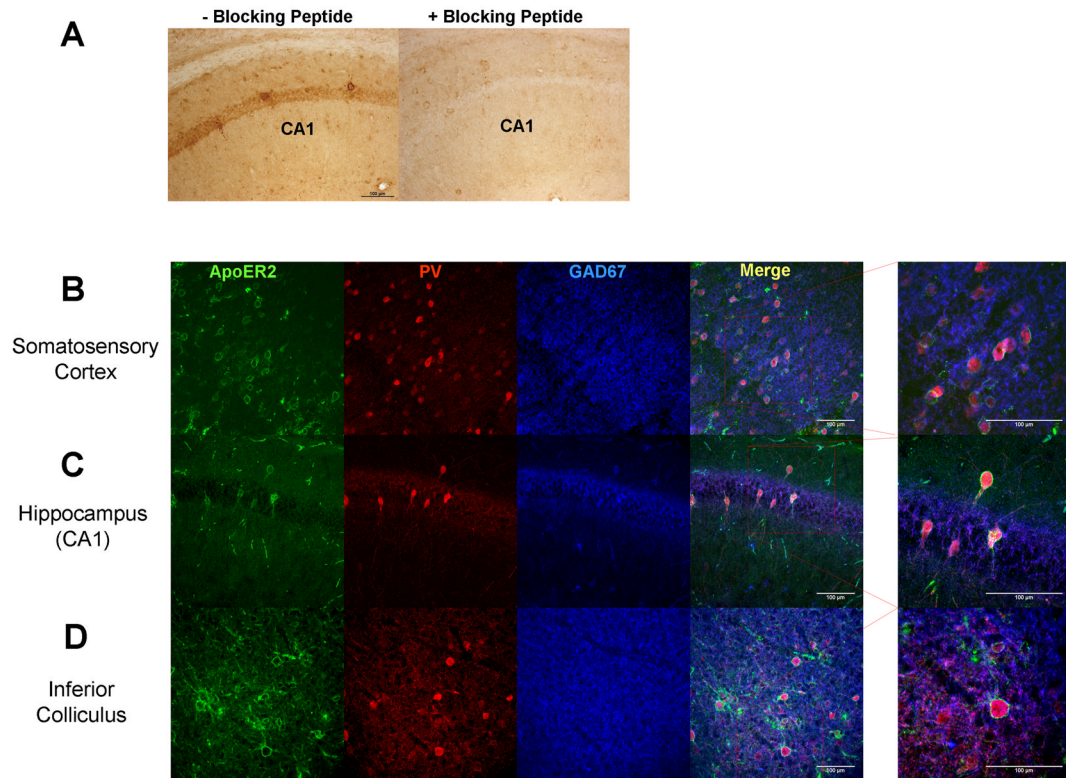
Figure 1.
ApoER2 is expressed on PV-interneurons. *A,* Images of CA1 region of the hippocampus probed with an ApoER2 antibody in the absence (left panel) and presence (right panel) of an ApoER2 blocking peptide which left only background staining. *B, C, D,* Confocal images showing the expression of ApoER2 (left), PV (middle left), GAD67 (middle right), and colocalization of the markers (right) in the somatosensory cortex (*B*) hippocampus (*C*), and inferior colliculus (*D*) of WT mice. Higher magnification of merged images (far right). Scale bar: 100 μm.
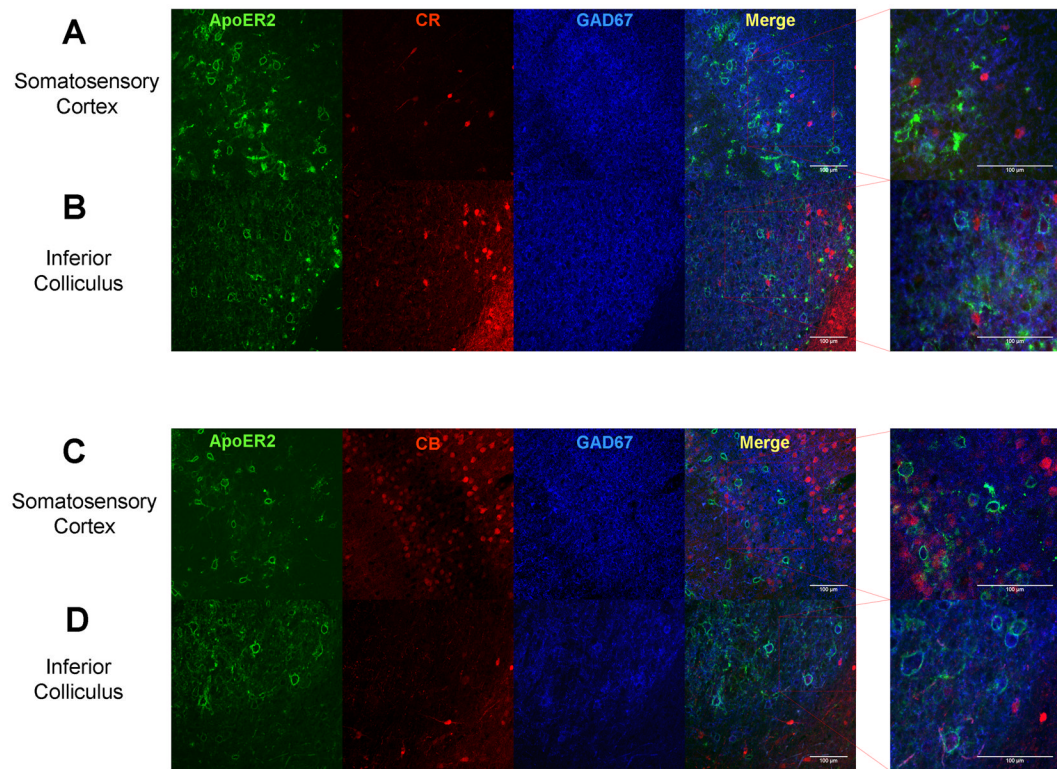
Figure 2.
ApoER2 is not expressed on calretinin (CR)-interneurons or calbindin (CB)-interneurons. *A, B, C, D,* Confocal images showing the expression of ApoER2 (left), CR (*A, B*) or CB (*C, D*) (middle left), GAD67 (middle right), and colocalization of the markers (right) in the somatosensory cortex (*A, C*) and inferior colliculus (*B, D*) of WT mice. Higher magnification of merged images (far right). Scale bar: 100 µm.
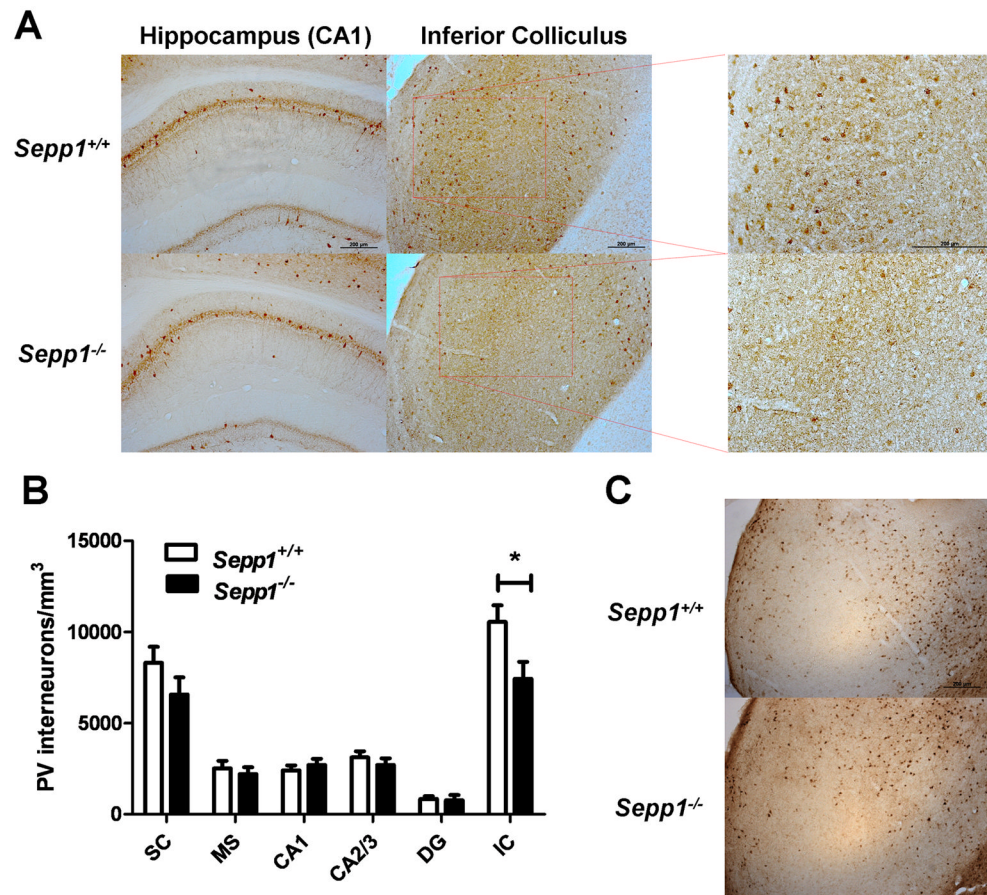
Figure 3.
Reduced density of PV-interneurons in *Sepp1*^{−/−} mice. *A,* Representative images showing PV expression in the hippocampus (left column), and inferior colliculus (middle and right columns) of WT *Sepp1*^{+/+} (top row) and *Sepp1*^{−/−} (bottom row) mice. Higher magnification images of the inferior colliculus (far right) *B*, Mean density of PV-interneurons per mm^3 (± SEM, n=6 per genotype) in brain regions investigated: somatosensory cortex (SC); medial septum (MS); dentate gyrus (DG), CA1 and CA2/3 of the hippocampus; inferior colliculus (IC). *p<0.01. *C*, Representative images showing CR expression in the inferior colliculus of WT *Sepp1*^{+/+} (top row) and *Sepp1*^{−/−} (bottom row) mice. Scale bar: 200 μm.
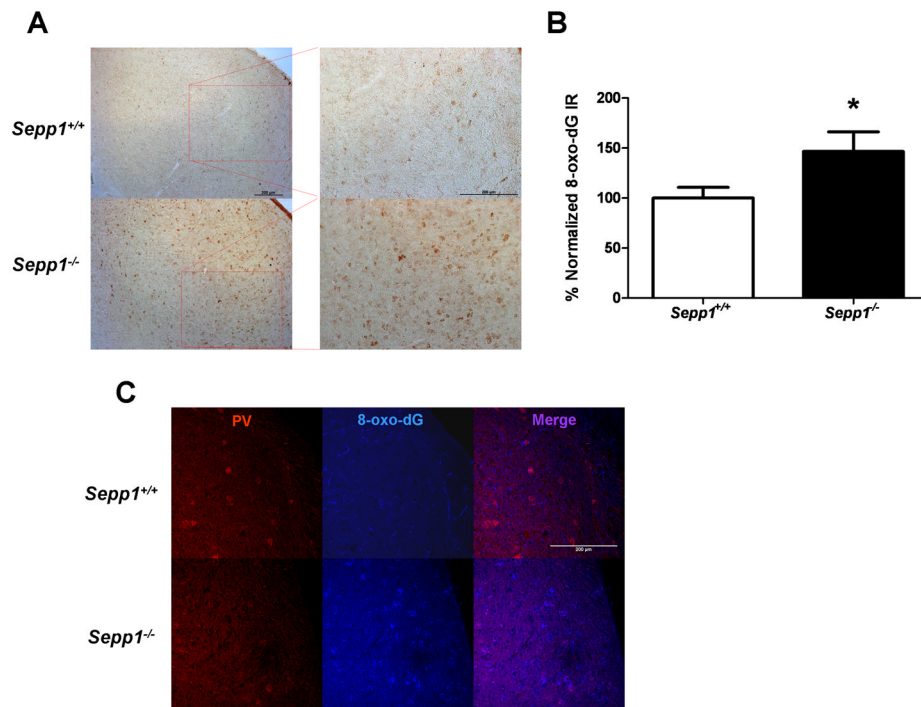
Figure 4.
Increased oxidative stress in the inferior colliculus of $Sepp1^{-/-}$ mice. **A**, Images of the inferior colliculus from WT $Sepp1^{+/+}$ (top row) and $Sepp1^{-/-}$ (bottom row) mice probed with an antibody for 8-oxo-dG and visualized with DAB staining. Higher magnification images (right) **B**, Normalized optical density measurements for 8-oxo-dG immunoreactivity in the inferior colliculus. *p<0.05. **C**, Confocal images (20x) showing PV (left), 8-oxo-dG (middle), and colocalization of the markers (right). Scale bar: 200 µm.
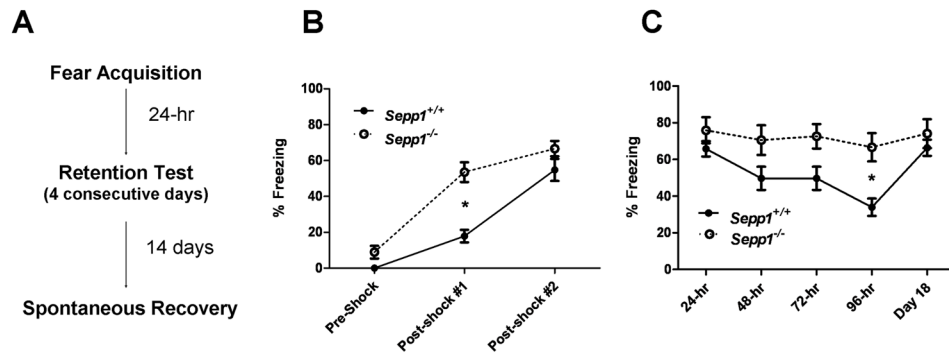
Figure 5.
Enhanced acquisition and impaired extinction of contextual fear in *Sepp1*$^{-/-}$ mice. *A,*
Contextual fear conditioning procedure. *B,* Mean (± SEM) percent contextual freezing
before and after each 2-min post-shock acquisition trial. *p<0.001. *C,* Mean (± SEM)
percent contextual freezing during fear retention testing. *p<0.01.

Figure 6.
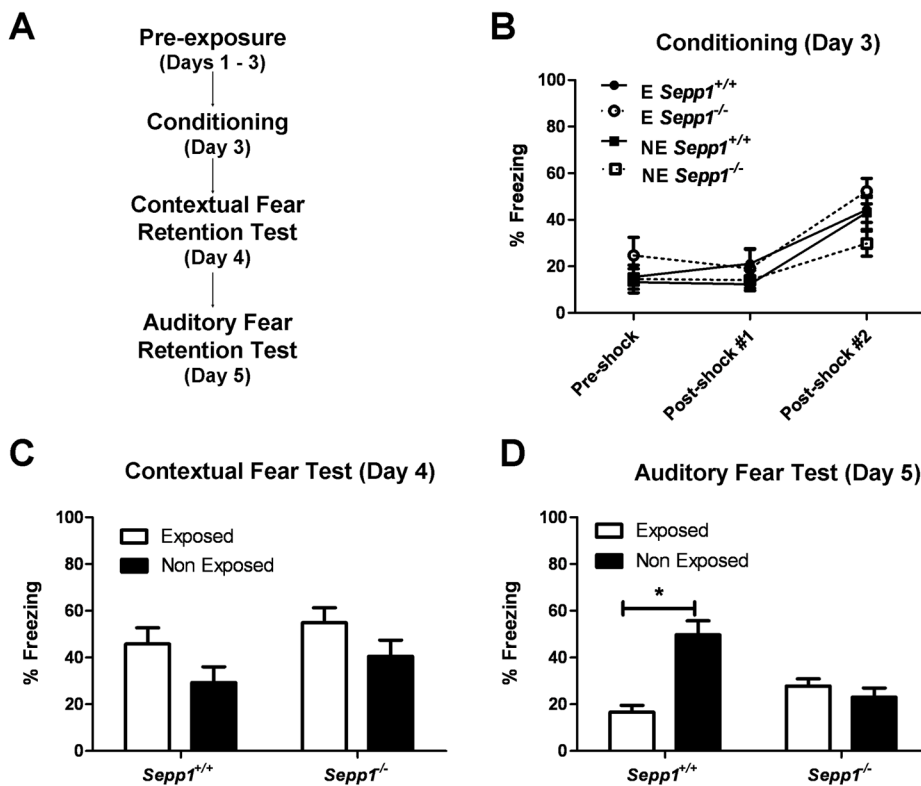Absence of latent inhibition in *Sepp1*$^{-/-}$ mice. *A*, Latent inhibition conditioning procedure. *B*, Mean (± SEM) percent contextual freezing before and after each 2-min post-shock acquisition trial (Day 3). *C*, Mean (± SEM) percent freezing during contextual fear retention testing (Day 4). *D*, Mean (± SEM) percent freezing during auditory fear retention testing (Day 5). *p<0.001.
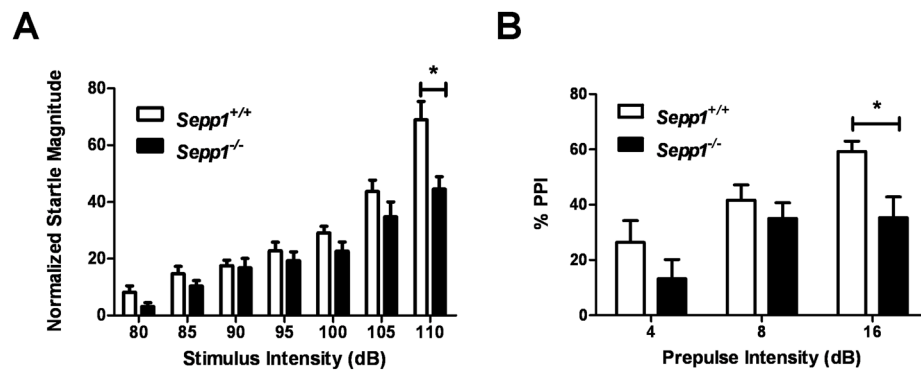
A

B

Figure 7.
Diminished acoustic startle reactivity and prepulse inhibition in *Sepp1*^{−/−} mice. *A,* Mean (± SEM) normalized startle magnitude as a function of acoustic stimulus intensity. *$p < 0.001$. *B,* Mean (± SEM) percentage of prepulse inhibition as a function of prepulse intensity above the background level (70 dB). *$p < 0.05$.
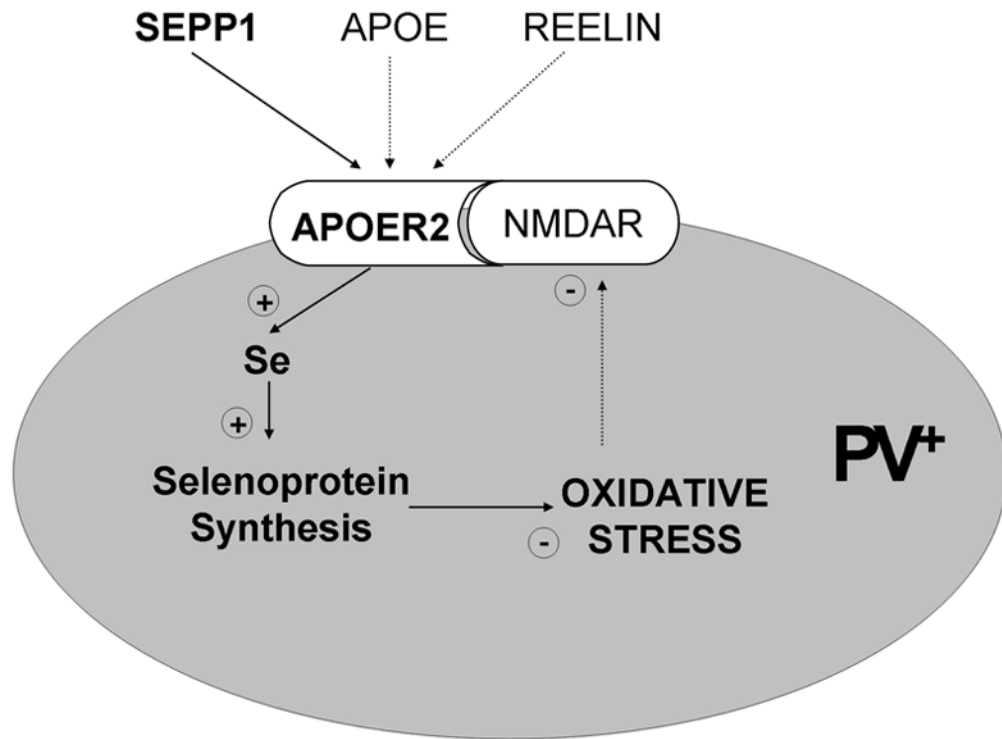
Figure 8.
Putative model of PV-interneuron function and oxidative stress. Sepp1 binds to ApoER2 and provides selenium for selenoprotein synthesis. Selenoproteins protect against oxidative stress. Oxidative stress impairs NMDA-mediated neurotransmission and, in turn, leads to diminished PV expression. Also included in this model, but beyond the scope of this investigation, are two additional ligands for the ApoER2 receptor, APOE and reelin.